Carbohydrate Polymer Technologies and Applications 5 (2023) 100328

Contents lists available at ScienceDirect

Carbohydrate Polymer Technologies and Applications

journal homepage: www.sciencedirect.com/journal/carbohydrate-polymer-technologies-and-applications

Development and characterization of starch-based bioactive thermoplastic packaging films derived from banana peels

Chandra Mohan Chandrasekar [a,*], Harini Krishnamachari [b], Stefano Farris [a], Diego Romano [a]

[a] Department of Food Environmental and Nutritional Sciences, University of Milan, Italy
[b] Centre for Food Technology, Anna University, India

ARTICLE INFO

Keywords:
Biopolymer
Banana peel starch
Banana peel
Nanocellulose fibers
Thermoplastic films
Bioactive packaging

ABSTRACT

The present work deals with the development of cellulose-reinforced starch-based bioactive thermoplastic packaging films, from complete recycling of banana peel waste. The nanocellulose fibers, starch and bioactive compounds from banana peel were extracted and reconstituted to produce cellulose-reinforced starch-based bioactive thermoplastic packaging films. The banana peel starch was examined to have an abundance of amylopectin (88.55 ± 0.28% (w/w)) and high thermal stability (~295 °C maximum degradation temperature), to serve as a matrix for the thermoplastic films. The ethanolic extract of the banana peel with major active compounds of β-sitosterol, and 1, 2 Benzenedicarboxylic acid mono (2-ethyl hexyl ester) was examined to be having high antioxidant (74.43 ± 0.26% DPPH inhibition) and antimicrobial properties, to serve as a potential bioactive ingredient for the development of bioactive thermoplastic films. The addition of banana peel-based nanocellulose fiber improved the mechanical (6-fold increase in tensile strength) and barrier properties (0.6-fold reduction in O_2 permeability) of banana peel thermoplastic films (BPT). The developed bioactive BPT films were examined to have a UV blocking capacity of ~98%. The produced Bioactive BPT films were found to be effective in the shelf life extension of bread by 10 days. The proposed methodology for the complete recycling of banana peel will take the state of research in agro-waste management one step closer to a green bio-circle economy.

1. Introduction

Generally, plastic wastes are difficult to dispose of due to their non-degradable nature. Furthermore, massive amounts of plastic waste are dumped into the environment every year, causing environmental pollution. In recent years, numerous researchers worked on the treatment of petro-plastics accumulation, but a complete solution to waste plastic disposal has not been found (Yuliana et al., 2012). Researchers are very much focused on finding eco-friendly biodegradable plastics to replace petroleum plastics as a solution to environmental pollution (Hassan et al., 2020). Biodegradable plastics will have more demand in the forthcoming years. Raw materials such as proteins, polyesters, lipids, and polysaccharides can be used for biodegradable plastic production. They are abundantly available in different agricultural resources. The compositions may be varied among the agricultural resources, which may result in variations in bio-thermoplastic properties.

Polysaccharides are a vital driving force in bioplastic research. Cellulose and starch are important bio-macromolecules in bioplastic production and research, because of their high abundance in nature (Czaikoski et al., 2020). The starch molecules consist of both crystalline linear polymer in amylose and amorphous branched polymer in amylopectin. Therefore, it can be a potential matrix for the development of bio-thermoplastics (Wilpiszewska & Czech, 2014). The cellulose molecules, mainly consist of a highly crystalline linear arrangement of β - glucose; thus, it can be a potential reinforcing material for starch-based bio-thermoplastic films. Recent studies in the blending of cellulose with synthetic polymers have revealed its superior reinforcing capacity, improving its synergistic thermal properties (Deepa et al., 2016; Iyer et al., 2016; Maya et al., 2017). In recent years, the extraction of nanocrystalline has gained a profound interest among researchers. It is due to the possible wide variety of industrial applications that can be developed from the unique physical and chemical properties of nano-crystalline cellulose fibers (Khalil et al., 2012; Kumar et al., 2014; Li et al., 2015). These unique characteristics of nanocrystalline cellulose fibers have influenced cellulose-reinforced starch-based bio-thermoplastics. We have recently developed and optimized a

* Corresponding author at: Department of Food Environmental and Nutritional Sciences, University of Milan, Italy.
E-mail address: chandra.chandrasekar@unimi.it (C.M. Chandrasekar).

https://doi.org/10.1016/j.carpta.2023.100328

Available online 29 May 2023

sustainable method for nanocrystalline cellulose fibers extraction (Harini et al., 2018). Bananas are a vital fruit plant in the world. Every part of the banana is beneficial, and they are also rich in bio-macromolecules (starch and cellulose) (Tibolla et al., 2014). The banana processing industries produce tons of banana peels as waste and disposal of these wastes are problematic. Peels of Banana are rich in cellulose and starch, which can be utilized as a potential resource to extract nanofibers of starch and cellulose (Tibolla et al., 2014, 2018). Furthermore, these wastes are also rich in many bioactive compounds (Nagarajaiah et al., 2011). These bioactive compounds are a potential active ingredient to develop active bio-thermoplastic packaging materials.

As a part of developing Bio circle economy from Banana Peel (BP). We hypothesize that the separation and reconstitution of biopolymers (starch and cellulose) from BP with BP active compounds will facilitate the production of Bioactive thermoplastics. Therefore, this study aims to extract the bioactive compounds, and starch from banana peel and explore the possibility of developing cellulose-reinforced starch-based bioactive thermoplastic packaging films (BPT). The effectiveness of the Bioactive BPT films were evaluated with shelf-life analysis of bread samples.

2. Materials and methods

2.1. Raw materials

Banana peels were collected from the banana processing industries in Chennai, Tamilnadu, India. For the preparation of banana peel powder, a fluidized bed dryer was used to dry the sample at 50 °C and then milled. The chemical compositions of raw banana peel powder were investigated as per the methods used in our previous studies. The nanocrystalline cellulose fibers produced from the banana peel in a previous study were used in this study for the reinforcement of BP starch films (Harini et al., 2018). The chemicals are supplied by Merck Millipore (Merck Specialties Pvt. Ltd.). Purity: EMPARTA^{ACS} grade was used for the experiments. Materials required for microbial culturing were procured from Hi-media laboratories.

2.2. Extraction of active compounds

Finely powdered banana peel (15 g) was separately blended for 2 min with a quantity of 100 mL solvents [Ethanol (E) and Hexane (H)]. These mixtures were kept in a shaker (Sub Zero, India) at room temperature for 16 h, then filtered using Whatman no. 1 filter paper. The filtered residues were collected and stored separately for starch/cellulose extraction. The filtrate was further centrifuged at 6000 rpm (Thermo Scientific, USA) for 10 min to remove micro residues. Then the clear extracts were membrane filtered (0.45 μm) and then concentrated in the rotary evaporator. The dried banana peel extracts of ethanol (E) and hexane (H) stored were at −20 °C for further analysis.

2.2.1. Characterization of active compounds

2.2.1.1. Antioxidant analysis of active extracts. Antioxidant capacities of the banana peel extract were evaluated by DPPH, TPC, ABTS, and FRAP analysis, as reported in our previous studies (Harini et al., 2018).

2.2.1.2. Antimicrobial analysis of active extracts. The paper disk diffusion method was used to assess the antimicrobial efficiency and minimum inhibition concentration of the ethanol and hexane extract of the banana peel. For antibacterial activity, bacterial cultures were adjusted to 0.5 McFarland turbidity standards. The Muller Hinton (MH) agar media was poured and solidified in Petri plates. The 100 μL of inoculum was spread onto the solidified media using a sterile spreader. Then the paper discs were impregnated with 100 μL solution having 1 mg/mL of extract and placed on agar plates. Paper discs impregnated with 100 μL of solvents were used as a negative control. The plates were stored for 18 h at 37 °C to evaluate antimicrobial properties by measuring the zone of inhibition around each paper disk.

2.2.1.3. Gas chromatography and mass spectroscopic analysis of active extracts. GC–MS analysis of banana peel extract was performed using an Agilent-6890 N gas chromatographer with an HP 5973 mass spectrometer detector (Radha Krishnan, 2015). The identification of compounds in the extracts was made by correlating mass spectra and retention times with that of pure compounds. Furthermore, the NIST (National Institute of Standards and Technologies, USA), mass spectra library, was also used for this analysis.

2.3. Extraction of starch and nano cellulose from banana peel

2.3.1. Extraction of starch

Isolation of the Starch was performed using the procedure reported in a previous study (Yuliana et al., 2012). The banana peel powder and water were mixed in a 1:5 ratio (w/w); soaked at 30 °C for 3 h and then blended for 5 min. This mixture was screened *via* a 60-mesh sieve to separate the filtrate and the residue. The collected residue was further mixed with 50 mL of ethanol (70%) for 5 min and filtered to separate the residue. The collected residue was blended for 5 min in 50 mL 0.1 M NaOH solution and again screened to collect the solid residue. This solid residue was used for nanocellulose extraction, as described in Section 2.3.2. The mixture of filtrates collected from all steps was centrifuged at 11,000 rpm in a centrifuge (Thermo Scientific, USA) for 15 min. The supernatant was decanted carefully, and the resultant was mixed with water (100 mL), filtered twice using a 200-mesh screen and Whatman filter paper (2.5 μm pore size & no.5). Further, it was washed consecutively with 0.1 M sodium hydroxide and deionized water. The filtered residue was dried in a freeze drier and dried starch was stored at −5 °C for further analysis.

2.3.2. Extraction of nanocellulose

The dried residue of banana peel powder after starch extraction was used to extract nanocrystalline cellulose fiber. As mentioned above in the materials section, we used the nanocrystalline cellulose extracted in our previous study.

2.4. Characterization of banana peel starch

The amylose and amylopectin composition of banana peel starch was examined as per the method defined in our previous study (Chandra Mohan et al., 2018).

2.4.1. Scanning electron microscopic analysis

The microstructure of starch and BPT film was observed by scanning electron microscope (HITACHI-S3400N, Japan). Before the analysis, samples were positioned on a stub with double side adhesive tape, positioned horizontally at an angle of 90° The sample was assessed using an accelerating potential of 20.0 kV (Sudharsan et al., 2016).

2.4.2. FTIR analysis

FT-IR spectra of banana peel starch were recorded using the Perkin Elmer FT-IR spectrometer (Perkin-Elmer Co., USA). Sample (0.3–0.5 mg) was mixed with potassium bromide (~ 0.5 g), and pressurized to make pellets (13 mm dia). The spectrum of samples was examined at the wavelength between 4000 and 400 cm^{-1} with a resolution of 4 cm^{-1} (Weligama Thuppahige et al., 2023).

2.4.3. X-ray diffraction analysis

The wide-angle X-ray diffraction measurement was carried out using D8 Advance Bruker AXS X-ray powder diffraction using a one-dimensional Debye–Scherr camera, Cu Ka radiation (wavelength

0.1542 nm) operating at 40 kV and 35 mA. The crystallinity index (CI) was calculated using Eq. (1), by measuring the peak height of the crystalline region (I_{cry}) and the amorphous region (I_{am}) (Acharya et al., 2017; dos Santos et al., 2016).

$$CI(\%) = \frac{I_{cry}}{I_{total}} \times 100\% \quad (1)$$

Where, I_{total} – Total area under XRD peaks [$I_{total} = I_{cry} + I_{am}$]

2.4.4. Thermal analysis

TGA analyses were performed on Universal V4.4A TA Instruments (CLRI, Chennai, Tamil Nadu). About (10 ± 3) mg of starch was placed in alumina pans. Samples were heated in a nitrogen atmosphere (sample flow - 60 mL/min and balanced flow - 40 mL/min) from ambient temperature to 800 °C, to create pyrolysis conditions. A heating rate of 5 °C/min was used to heat the sample.

DSC measurements were carried out on Perkin Elmer Pyres 1 DSC. Each sample (5–10 mg) was first heated to 200 °C under the protection of nitrogen at a flow rate of 20 mL/min. Then, it was immediately cooled with liquid nitrogen to −50 °C. The sample is then scanned at a heating rate of 10 °C/min. The results were recorded from −50 °C to 300 °C. All samples used in the experiments were in powdered form. DSC of the samples was carried out in CLRI, Chennai, Tamil Nadu (Warren et al., 2016).

2.5. Preparation of banana peel starch thermoplastic packaging films

The film-forming solution containing banana peel starch (7.5%), citric acid (1.2%), varying concentrations of nanocellulose (1% - 5%), and distilled water (100 mL) was stirred in a shaker for 20 mins. All the films were made by casting method, 30 mL of film matrix solution was poured onto Petri dishes (15 cm in diameter) and dried at 40 °C for about 24 h in an incubator. The dried films were peeled off from Petri plates and stored for further analysis.

2.6. Characterization of banana peel starch thermoplastic films

2.6.1. Mechanical properties

The tensile and elongation properties of the films were determined in a Texture Analyzer TA. XT Plus (Stable Micro Systems) with a tensile grip probe. The film samples were cut as rectangular strips (3 cm x 7 cm) and positioned in the film-extension grips of the texture testing machine. Film samples were stretched at a rate of 50 mm/min until breaking. A microcomputer was used to log the stress-strain curves. For each film, a minimum of three replicate tests were performed. Results of Tensile strength were expressed in Mpa and elongation at break as in% (Saberi et al., 2017). Young's modulus/elastic modulus of the material was also calculated.

2.6.2. Oxygen transfer rate

The rate of oxygen transmission was estimated using an Ox-Tran modular system at 50 ± 1% RH and 23 °C. Before testing, samples were equilibrated for 48 h at 50 ± 1% RH (23 ± 1 °C). The film samples were positioned on a stainless-steel mask with an open test area of 5 cm^2. The film was exposed to oxygen gas (100%) on one side and 98% N_2 and 2% H_2 on the other side. Nitrogen gas was connected to the colorimetric sensor, and measurements were taken when a steady state was reached. To control the relative humidity of both gases, a humidifier was used and RH varied between 50 and 90%. At low RH levels (below 50%), permeability analysis was not performed as starch films begins to crack. The rate of oxygen permeation was estimated by dividing the O_2 transmission rate by the difference in O_2 partial pressure on both sides of the film (101 kPa) and multiplying by the average thickness of the film (μm) (Ghasemlou et al., 2013a).

2.6.3. Color and light transmission analysis of banana peel packaging films

The color parameters (L, a, and b) of the film samples were measured using a Hunter Lab colorimeter (Radha Krishnan, 2015). The tests were performed with an opening of 14 mm and a 10° standard observer. The calibration of colorimeter was done using a standard white tile (L* = 93.49, a* = −0.25, b* = −0.09). At three different points (randomly) samples were analyzed in colorimeter.

The transparency of the film samples was measured in a spectrophotometer method explained by Han and Floros (1997). The rectangular film (4 × 10 mm) was placed in a spectrophotometer cell and recorded the film's light transmittance at 600 nm. The following equation calculated transparency:

$$\text{Transparency} = \frac{\log\%T}{b} \quad (2)$$

Where%T was the light transmittance at 600 nm, and b was the thickness of the film (mm).

2.6.4. Moisture content of films

The moisture content of films was calculated based on weight loss in films after drying them in an oven at 110 °C until a constant dry weight was attained.

$$\%\ \text{Moisture} = 100x\frac{W_1 - W_0}{W_2 - W_0} \quad (3)$$

Where,

W_1 = weight in g of a dish with the powdered sample; W_2 = weight in g of a dish with ash

W_0 = weight in g of the empty dish

2.6.5. Solubility test for films

The film solubility was determined by a method adapted from Ghasemlou et al. (2013a). The initial weight of film samples was recorded after cutting them into small pieces (4.0 cm^2 size). The samples were immersed in distilled water (100 mL) and shaken for 10 min at 180 rpm at 25 °C. Finally, films were taken and dried in a hot air oven at 110 °C till constant weight was reached. The solubility of the film (%) was calculated by using the following equation,

$$WS(\%) = \left[\left(W_0 - W_f\right) / W_0\right] \times 100 \quad (4)$$

Where,

W_0 - The initial film weight expressed as dry matter

W_f - The weight of the final desiccated un-dissolved film

2.6.6. Atomic force microscopy

Atomic force micrographs (AFM) of developed film samples were taken at contact mode using Park XE-100 AFM (Park Systems, Korea). Multiple measurements were taken for the area over the film surface (50 × 50 μm). Statistical parameters: Average maximum roughness valley depth (Rvm), root mean square roughness (Rq), average roughness (Ra), and Average maximum height of roughness (Rtm) were taken up to estimate the roughness of films quantitatively.

2.6.7. UV transmission analysis

The UV transmission spectra of BPT films were analyzed using UV–VIS Spectrophotometer in the wavelength range between 200 and 400 nm. The samples were cut into 1 × 3 cm size films for analysis. The UV protection percentage of the films for UVA (315–400 nm) and UVB (280–315 nm) were calculated using the following formulae (Shao et al., 2022).

$$UVA\ blocking\ (\%) = 100 - \frac{\int_{315}^{400} T(\lambda)d(\lambda)}{\int_{315}^{400} d(\lambda)} \times 100 \quad (5)$$

$$UVB\ blocking\ (\%) = 100 - \frac{\int_{280}^{315} T(\lambda)d(\lambda)}{\int_{280}^{315} d(\lambda)} \times\ 100 \quad (6)$$

2.7. Shelf-life analysis of bread

The bread samples were made from the freshly prepared dough without adding any chemical preservatives and baked at 180 °C for 40 min. The samples were cooled, sliced and packed into the Polyethylene (PE), BPT and Bioactive BPT films. Then the packed bread samples were stored at 4 °C (Fig. 1). The samples stored inside PE films were taken as control.

The packed samples were analyzed for its Moisture Content (Oven method), Water Activity (AquaLab water activity meter, Meter Group Inc., USA) (Chang et al., 2023), Texture (TA.XTplus, Stable Micro Systems, UK equipped with 36 mm cylinder probe and 5 kg for estimation of bread firmness), Color (Hunter colorimeter, HunterLab, USA), Acidity (Titration method), Total Plate Count and (Yeast and Mold) Count (Chang et al., 2023; Petchwattana et al., 2021).

2.8. Statistical analysis

All the analyses were performed in triplicates, and average values with standard deviation values are reported. The One-way Analysis of the Variance (ANOVA) test and Duncan's multiple range test were performed for the mean values of analyses to evaluate the statistically significant differences, with a confidence level of 95% ($P \leq 0.05$). Microsoft Excel Data Analysis centre (2010) and IBM SPSS software (version 22) were used for the statistical data analysis.

3. Results and discussions

3.1. Extraction and characterization of active compounds from banana peel

The yield of active compounds from banana peel was estimated to be 20.17 ± 0.43 and 15.31 ± 0.29% (w/w) in the solvents of ethanol and hexane.

3.1.1. Antioxidant and antimicrobial properties of banana peel extract

The antioxidant and antimicrobial characteristics of banana peel extracts are shown in Table 1. The ethanolic extract of banana peel was examined to have considerably ($P < 0.05$) high antioxidant and antimicrobial capacity compared with hexane extract. This high antioxidant and antimicrobial activity of ethanolic extract may be attributed to the high phenolic content present in banana peel, which is polar (Hassan et al., 1970; Mordi et al., 2016). Sakkas and Papadopoulou extensively studied the mechanism of active phenolic compounds against microbes (Sakkas & Papadopoulou, 2017). They stated that the antimicrobial activity of phenolic compounds could not be accredited to a single mechanism but to several different mechanisms at different locations in bacterial cells, external and internal components that affect enzymes, ions, cytoplasm, cell membranes, proteins, fatty acids, and metabolites. The overall minimum inhibitory concentration (MIC) of the BP ethanolic extract was examined to be 150 μg/mL, estimated against the growth of *Pseudomonas aeruginosa*. The observed high MIC could be because of the high resistance of *Pseudomonas aeruginosa* to active compounds present in the banana peel extract. Since the BP ethanolic extract's overall activity was examined to be high, it was subjected to further chemical composition analysis through gas chromatography-mass spectrometry.

3.1.2. Chemical composition of banana peel extract

Fig. 2, illustrates the GC–MS chromatogram of banana peel ethanolic extract. Table 2, tabulates the chemical composition of banana peel ethanolic extract, estimated using peak area calculation from GC–MS chromatogram. The chemical constituents of the BP ethanolic extract were examined to be rich in β- sitosterol (31.30%), and 1, 2-Benzenedicarboxylic acid mono (2-ethyl hexyl ester) (12.47%). Ododo et al. (2016) and Sen et al. (2012) studied the antimicrobial capacity of β-sitosterol and stated that the mechanism of action for its superior antimicrobial activity could be ascribed to the disruption of microbial cell walls to induce cell death. Jafari et al. (2017) stated that the antimicrobial mechanism of 1,2-Benzenedicarboxylic acid mono (2-ethyl hexyl ester) might be because of the release of protons to affect the receptors present in the cell wall of microbes. Other compounds, such as β-tocopherol (10.33%) and Estragole (10.18%), were also examined to be present in BP extract.

3.2. Extraction and characterization of BP starch

Table 3, tabulates the composition of raw banana peel powder and extracted banana peel starch. The banana peel was rich in cellulose and starch content. The extraction yield of starch was 28.24 ± 0.68% (w/w). The extracted banana peel starch was observed to be rich in amylopectin. Therefore, it was observed to be moderate amylose starch (10 – 30% amylose content). Amylopectin plays a significant role in binding linear polymers to give flexible packaging material (Ferreira et al., 2020). The presence of a higher percentage of branched amorphous amylopectin in BP starch may be suitable for the development of stable thermoplastic material. The nanocellulose fibers extracted in our initial study were used to produce bioactive thermoplastic films (Harini et al., 2018).

3.2.1. Thermal analysis of BP starch

Fig. 3, shows the thermogravimetric assessment of extracted banana

Fig. 1. A) Bread sample packed in PE films, B) Bread sample packed in BPT film, C) Bread sample packed in Bioactive BPT film.

Table 1
Antioxidant and antimicrobial analyses results for banana peel extracts.

Banana peel extracts	Antioxidant analyses				Antimicrobial analyses					
	DPPH	TPC	ABTS	FRAP	*LM*	*SA*	*EC*	*PA*	*KP*	*SE*
Units	% Inhibition	mg of GAE/g	μmol TE/g	μmol TE/g	Zone of inhibition (mm)					
Ethanol (E)	74.43 ± 0.26	82.27 ± 0.31	9.54 ± 0.62	12.55 ± 0.35	12.26 ± 0.13	8.24 ± 0.25	16.32 ± 0.31	5.68 ± 0.29	16.34 ± 0.38	20.47 ± 0.52
Hexane (H)	31.22 ± 0.51	25.17 ± 0.37	2.14 ± 0.23	2.31 ± 0.26	3.11 ± 0.17	2.62 ± 0.14	3.27 ± 0.24	1.61 ± 0.18	4.34 ± 0.23	4.23 ± 0.27
MIC-E (μg/mL)	–	–	–	–	50	100	50	150	50	50
MIC—H (μg/mL)	–	–	–	–	100	100	150	200	150	100

Abbreviations: **DPPH** - 2,2-diphenyl-1-picrylhydrazyl scavenging activity; **TPC** – Total phenolic content; **ABTS** - 2,2′-azino-bis(3-ethylbenzothiazoline-6-sulphonic acid) scavenging activity; **FRAP** - Ferric reducing antioxidant power; ***LM*** **-** *Listeria monocytogenes;* ***SA*** **-** *Staphylococcus aureus;* ***EC*** **-** *E. coli;* ***PA*** **-** *Pseudomonas aeruginosa;* ***KP*** **-** *Klebsiella pneumonia;* ***SE*** **-** *S. enteritidis.*

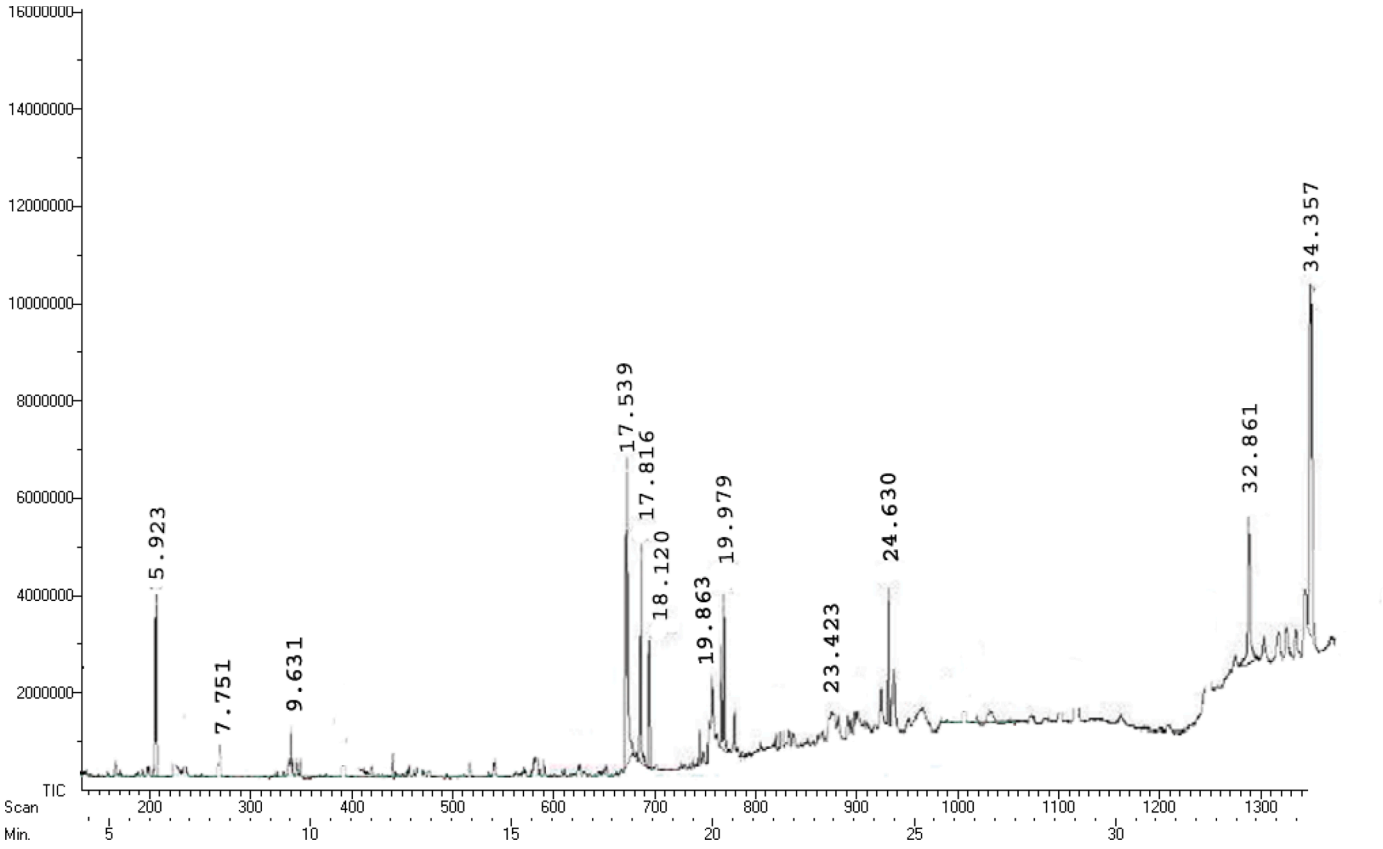

Fig. 2. GC–MS chromatogram of banana peel ethanolic extract.

peel starch. The initial mass loss of banana peel starch occurred below 100 °C; this could be because of the initial dehydration of starch (Eyholzer et al., 2010; Sahoo et al., 2005). The thermal degradation occurred with the most significant loss in weight (~41.99%) between 229.65 °C and 362.96 °C. This degradation may be caused by the breakdown of glucose rings in the polymer composition (amylose/amylopectin) of starch (Puncha-Arnon & Uttapap, 2013; Sui et al., 2016). The constant decomposition of banana peel starch was noted between 362.96 °C and 800 °C, after the second decomposition. The derivative weight loss curve of banana peel starch denoted the peak decomposition temperature of 295.69 °C. Fig. 4, depicts the differential scanning calorimetric curve of banana peel starch. Two endothermic peaks were observed on the DSC analysis of banana peel starch. The first endothermic peak at around 95.22 °C, corresponds to the evaporation of water molecules from the sample (Alamri et al., 2012). The main endothermic peak with energy absorption of 253.56 J/g was observed to be between 173.23 to 300 °C. This energy is required to degrade the banana peel starch molecules to break the linkages among and within glucose molecules (Weligama Thuppahige et al., 2023). Consecutively, the thermal analysis results of banana peel starch reveal that the BP starch molecules can be subjected to various processing conditions under 229.65 °C, with intact stability.

3.2.2. *FTIR spectroscopic analysis of BP starch*

FTIR spectra examine interactions between monomers to form polymers. Fig. 5, shows the FTIR spectrum of banana peel starch, which have a broad, intense band at 3287 m^{-1} corresponding to Hydrogen bonded polymeric OH stretch vibrations of starch (Coates, 2006; Czaikoski et al., 2020). The peak at 2917 cm^{-1} illustrates the occurrence of $–CH_2$ groups with C—H stretch (Wulandari et al., 2016). The fingerprint region of starch is between 600 and 1500 cm^{-1} (Weligama Thuppahige et al., 2023). The characteristic peaks of starch overlapped with each

Table 2
Chemical composition of banana peel ethanolic extract.

Chemical component	Retention time (min)	Peak area (%)	Molecular formula	Molecular weight (g/mol)
Estragole	5.923	10.18	$C_{10}H_{12}O$	148.20
4H-pyran-4-one	7.751	0.28	$C_5H_4O_2$	96.08
Benzoic acid	9.631	0.92	C_6H_5COOH	122.12
Hexadecanoic acid ethyl ester	17.539	9.77	$C_{18}H_{36}O_2$	284.5
Epicatechin	17.816	9.98	$C_{15}H_{14}O_6$	290.27
Gallocatechin	18.120	8.59	$C_{15}H_{14}O_7$	306.27
Octadecanoic acid	19.863	1.65	$C_{18}H_{36}O_2$	284.50
p-coumaric acid methyl ester	19.979	4.29	$C_{10}H_{10}O_3$	178.18
9-Tricosene	23.423	0.24	$C_{10}H_{12}O$	322.60
1, 2 Benzenedicarboxylic acid mono (2-ethylhexylester)	24.630	12.47	$C_{16}H_{22}O_4$	278.34
Beta-tocopherol	32.861	10.33	$C_{28}H_{48}O_2$	416.70
Beta- sitosterol	34.357	31.30	$C_{29}H_{50}O$	414.71

Table 3
Composition of raw banana peel powder and banana peel starch.

Sample Banana peel Raw powder	Unit % (w/w)
Cellulose	44.04 ± 1.15
Starch	30.18 ± 1.22
Protein	1.10 ± 0.31
Lignin	8.08 ± 1.05
Hemicellulose	5.17 ± 1.03
Ash	7.85 ± 1.14
Others	2.58 ± 0.04
Extracted banana peel starch	**% (w/w)**
Amylose	11.45 ± 0.28
Amylopectin	88.55 ± 0.28

other in the fingerprint region and bands were observed at 1365, and 1005 cm^{-1} corresponding to the ring C—C stretch, and C—O-C glycoside linkages, respectively (Coates, 2006; Ferreira et al., 2020). The band at 1624 cm^{-1} corresponds to N—H primary amine bends of proteins associated with banana peel starch (Weligama Thuppahige et al., 2023). The codex standards accept the moisture (10 – 13.5%) and protein (3%) content of starch for its excellent quality (Algar et al., 2019).

3.2.3. *Crystallinity of BP starch*

Amorphous and crystalline layers are arranged in concentric rings inside the granule architecture of starch. The double helices of the amylopectin side chain are found in the crystalline domains. Some of the longer amylose chains may potentially interact with amylopectin through double helix interactions (Pérez & Bertoft, 2010). The crystalline polymorphs of starch molecules are classified into three types A, B and C (A mixture of A and B types) (Pozo et al., 2018). The diffractogram of banana peel starch showed distinctive peaks at 13.84, 21.88, 38.84, and 42.84° (Fig. 6). These characteristic peaks showed that isolated banana peel starch is a B-type starch. Hizukuri et al. (1983) stated that the degree of polymerization in branched amylopectin chains is related to the type of polymorphism in starch. Type B starch usually has a high percentage of long-chain polymers (Degree of Polymerization > 37), which correlates with the high intensity of the 1005 cm^{-1} band,

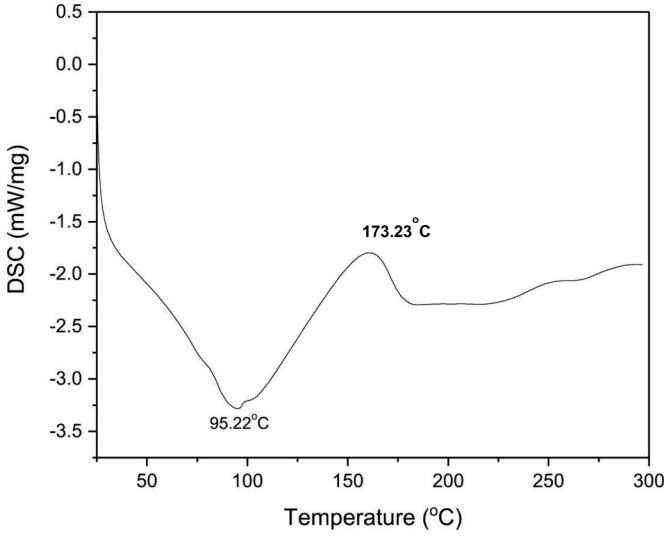

Fig. 4. Differential scanning calorimetric curve of banana peel starch.

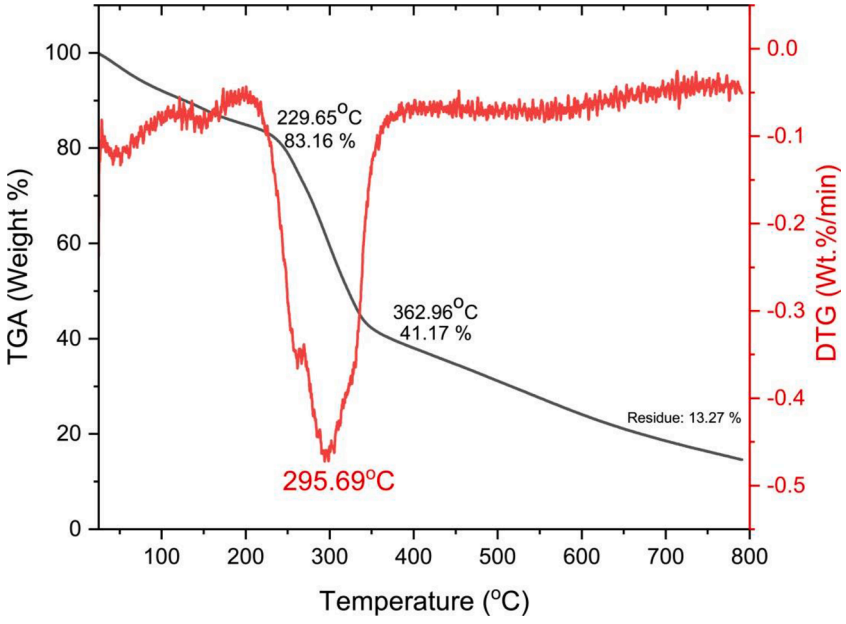

Fig. 3. Thermogravimetric curves of banana peel starch.

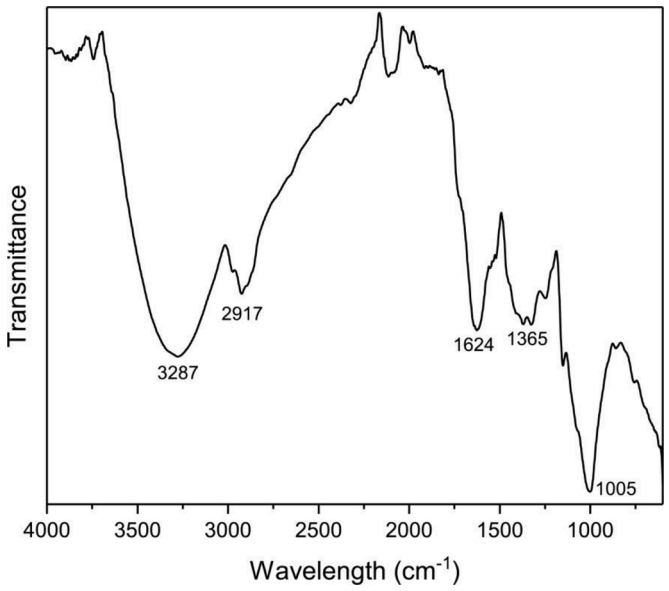

Fig. 5. Fourier transform the infrared spectral pattern of banana peel starch.

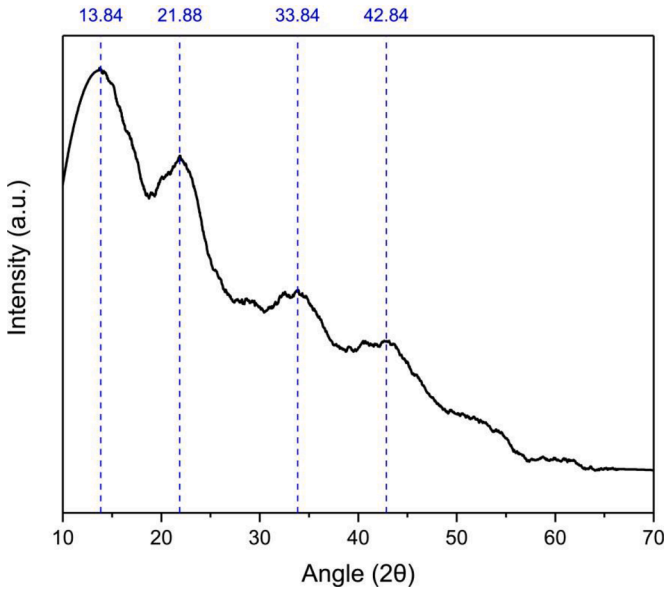

Fig. 6. X-ray diffractogram of banana peel starch.

corresponding to glycosidic linkages between glucose subunits (Huang et al., 2021). Van Soest et al. reported that the intensity of the 1022 cm^{-1} band in starch is inversely proportional to the amorphous state of starch (van Soest et al., 1995). Thus, the intensity ratio between the FTIR bands of 1044 and 1022 cm^{-1} is being used as an indicator for starch crystallinity (Pérez & Bertoft, 2010). The starch crystalline ratio of BP starch estimated using FTIR band intensities is 0.621. The crystallinity index of BP starch estimated through XRD is 22%, which indicates a high quantity of amorphous regions. This result is in agreement with the high amount of amylopectin noted in the proximate analysis of BP starch. This also attributes to the deformation of the starch structure during gelatinization, which may facilitate the formation of stable bio-thermoplastic material combined with other linear polymers and reinforcing agents (dos Santos et al., 2016; Veiga-Santos et al., 2005). The crystalline ratio of starch calculated from IR band intensities cannot be collaborated with the crystalline index of starch calculated from XRD, as the long-range order structures in starch (crystalline order) depend not only on short-range order interactions of double helices (Warren et al., 2016). Similar to BP starch molecules, potato starch molecules were also reported to have B-type starches, with CI ranges between 20 and 23% (dos Santos et al., 2016; Zobel, 1988).

3.2.4. *Surface morphology of BP starch*

Fig. 7 illustrates the scanning electron micrographs (SEM) of banana peel starch molecules. The starch molecules have an irregular globular structure. The size of the starch molecules was ranging from 1 μm to 3 μm in diameter. The starch molecule size plays a significant place in proper gelatinization and proper blending with the reinforcing agent (Ghasemlou et al., 2013b). Being small in molecular size, banana peel starch molecules may facilitate the proper gelatinization and blend for the development of thermoplastic packaging films.

3.3. *Preparation and characterization of BPT starch films*

The initial optimization studies have shown that less than 5% of starch is insufficient to produce stable packaging films. The reason may be inadequate interactions between amylopectin and amylose or less quantity of linear polymers in the film-casting solution. It has been found that even films formed with higher starch concentrations are brittle, attributed to the lack of plasticizing property in banana peel starch. So the optimized glycerol concentration (1.25%) was mixed into the film matrix solution, to increase their plasticization. The nanocellulose fibers from the banana peel were examined for their reinforcing capacity in the banana peel starch film. The BP starch-cellulose composite films were formed using cellulose treated with citric acid. Citric acid functions as a binding/cross-linking molecule between starch and cellulose to produce visually homogenized film solutions without any evidence of phase separation (Hassan et al., 2020).

3.3.1. *Mechanical and physical properties of BPT starch films*

The physical properties, oxygen transfer rate and mechanical characteristics of banana peel thermoplastic films are shown in Table 4. Oxygen permeability is the barrier property of the packaging films which is necessary to extend the shelf life of food products. A minor reduction in the banana peel starch film's oxygen transfer rate was observed with an increase in the concentration of starch (5 to 7.5%(w/v)) in the film matrix solution. The tensile strength of the BPT films increased considerably ($P < 0.05$) with an increase of starch concentration from 5 to 7.5%(w/v), a further increase in the concentration of starch has no significant effect on the tensile strength of the film. This reduction in OTR and tensile strength increase could be because of an increase in total solids of film matrix solution that may reduce

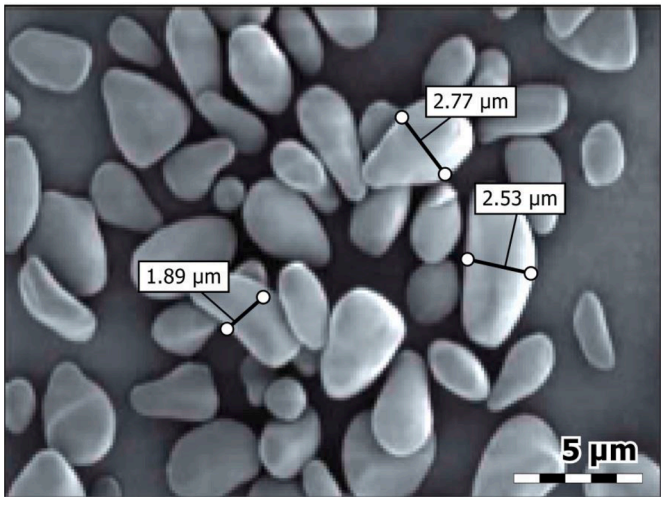

Fig. 7. Scanning electron micrographs of banana peel starch.

Table 4
Oxygen transfer rate, physical, and mechanical properties of BPT films.

Film Composition Units	Oxygen transfer rate $cm^3 \mu mm^{-2} d^{-1} kPa^{-1}$	Tensile strength MPa	Elongation at break %	Young's modulus MPa	Moisture uptake %
5% BP starch (BPS-5)	13.24 ± 1.13	3.76 ± 0.31	98.53 ± 2.00	3.81 ± 0.47	17.11 ± 0.13
7.5% BP starch (BPS-7.5)	12.70 ± 1.19[a]	5.10 ± 0.24[a]	101.51 ± 2.06[a]	5.02 ± 0.58	17.73 ± 0.35[a,c]
10% BP starch (BPS-10)	12.50 ± 1.10	5.29 ± 0.23	103.74 ± 1.63	5.09 ± 0.62	18.36 ± 0.31
BPS −7.5 + 1% BP-NCF (BPS - BP-NCF 1)	11.45 ± 1.38[b,a]	16.69 ± 0.59[b]	97.81 ± 2.68[b]	17.06 ± 0.68	16.96 ± 0.35[d]
BPS −7.5 + 2% BP-NCF (BPS - BP-NCF 2)	10.58 ± 1.35[b,b]	24.69 ± 0.85[b]	97.25 ± 2.58[b]	25.38 ± 0.72	15.99 ± 0.24[b]
BPS −7.5 + 3% BP-NCF (BPS - BP-NCF 3)	9.52 ± 1.22[b]	30.71 ± 0.61[b]	99.86 ± 3.22[b]	30.75 ± 0.76	14.95 ± 0.31[b]
BPS −7.5 + 4% BP-NCF (BPS - BP-NCF 4)	9.44 ± 1.35[b]	30.53 ± 0.45[b]	92.19 ± 2.67[b]	33.11 ± 0.53	14.89 ± 0.35[b]
BPS −7.5 + 5% BP-NCF (BPS - BP-NCF 5)	9.43 ± 1.43[b]	30.89 ± 0.81[b]	90.29 ± 2.56[b]	34.21 ± 0.46	14.85 ± 0.29[b]
	Solubility	**Color parameters**			**Light transmittance**
	%	**L**	**a**	**b**	**%**
5% BP starch (BPS-5)	44.45 ± 0.56	66.22 ± 0.35	5.94 ± 0.46	33.25 ± 0.41	9.53 ± 0.27
7.5% BP starch (BPS-7.5)	48.52 ± 0.35[a]	63.37 ± 0.24	5.98 ± 0.16	33.44 ± 0.35	9.23 ± 0.22
10% BP starch (BPS-10)	43.76 ± 0.36	65.25 ± 0.31	5.99 ± 0.11	34.35 ± 0.36	8.54 ± 0.14
BPS −7.5 + 1% BP-NCF (BPS - BP-NCF 1)	53.38 ± 0.36[b]	71.15 ± 0.23	5.38 ± 0.16	32.89 ± 0.79	9.45 ± 0.58
BPS −7.5 + 2% BP-NCF (BPS - BP-NCF 2)	53.56 ± 0.85[b]	69.96 ± 0.57	5.95 ± 0.24	33.98 ± 0.94	9.87 ± 0.41
BPS −7.5 + 3% BP-NCF (BPS - BP-NCF 3)	53.75 ± 0.27[b]	73.63 ± 0.51	4.77 ± 0.11	31.17 ± 0.56	9.44 ± 0.85
BPS −7.5 + 4% BP-NCF (BPS - BP-NCF 4)	54.28 ± 0.38[b]	72.26 ± 0.28	5.19 ± 0.17	32.13 ± 0.77	8.37 ± 0.57
BPS −7.5 + 5% BP-NCF (BPS - BP-NCF 5)	54.53 ± 0.86[b]	74.27 ± 0.68	5.27 ± 0.15	29.55 ± 0.49	8.97 ± 0.24

Results are expressed in Mean ± S.D.
[a - b], represents significant differences ($P < 0.05$) between values.
[c - d], represents no significant differences ($P > 0.05$) between values.

micropores in starch-based films to enhance its strength and barrier properties. Consecutively, a 7.5%(w/v) concentration of the BP starch solution, was selected for further reinforcement with nanocellulose fibers. The oxygen transfer rate of banana peel starch films considerably ($P < 0.05$) reduced when nanocrystalline cellulose was added. A significant reduction in OTR was noted with the further addition of nanocellulose fibers to 3%(w/v) reinforcement. The tensile strength of the BPT films also considerably ($P < 0.05$) increased from 5.10 ± 0.24 to 16.69 ± 0.59 MPa at 1%(w/v) BP-NCF reinforcement, 24.69 ± 0.85 MPa at 2%(w/v) BP-NCF reinforcement, and 30.71 ± 0.61 MPa at 3%(w/v) BP-NCF reinforcement. This significant improvement in OTR and mechanical characteristics of BPT films may be the deformation of low crystalline (~22% CI) amorphous regions of BP starch during gelatinization, which improves the interactions between starch, citric acid, and BP Nano cellulose molecules at a specific concentration (Wilpiszewska & Czech, 2014). Further increase in the concentration of nanocellulose may not have enough amorphous amylopectin molecules in starch to form stable BPT films. This may be the reason for the insignificant ($P > 0.05$) effect in OTR and mechanical properties above 3%(w/v) of Nano cellulose reinforcement. Upon the addition of nanocrystalline cellulose fibers, the moisture uptake of BPT films was examined to be significantly reduced. The reason may be the high crystalline nature of nanocellulose fibers. The solubility of BPT cellulose fibers was examined to be significantly increased with the addition of nanocellulose fibers. This phenomenon could be attributed to the improved interactions between cellulose, citric acid, and starch molecules to form a stable homogenized solution with the solvent. The color parameters and light transmittance of BPT films have no significant effect on the addition of nanocellulose fibers. There was only a slight reduction in the value towards the origin of the scale to indicate the addition of whiteness through cellulose, but the films remained pale yellow. It was evident from the above study that BPT starch films produced with a combination of 7.5%(w/v) BP starch and 3%(w/v) BP-NCF have a superior barrier and mechanical properties. Consecutively, BPS-BP-NCF 3 formulation of BPT film was selected for the infusion of banana peel active compounds.

3.3.2. *Surface morphology of BPT starch films*

Fig. 8, shows the scanning electron micrograph (A) and atomic force micrograph (B) of BPT films produced from a combination of 7.5%(w/v) BP starch and 3%(w/v) BP nanocellulose fiber. The scanning electron micrograph of the BPT film showed smooth surface morphology; this could be because of nanocellulose fiber in the nano range size facilitating proper interaction with amorphous regions of starch. The AFM of BPT films revealed the surface roughness parameters of BPT starch. The

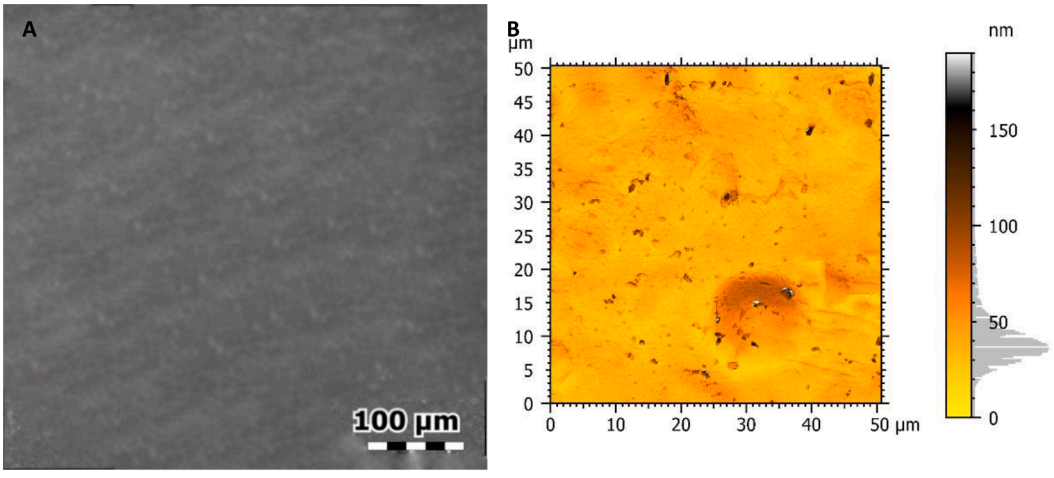

Fig. 8. Surface morphology of banana peel thermoplastic films [A – Scanning electron micrograph of BPT films; B – Atomic force micrograph of BPT films].

values of Rtm, Rvm, Ra, and Rq of BPT starch film were 149.57 ± 1.34, 40.42 ± 1.28, 9.00 ± 1.14, and 14.08 ± 1.21 nm, respectively.

3.3.3. XRD morphology and FTIR functional characteristics of thermoplastic films

The interaction between starch and nanocellulose molecules is responsible for improved mechanical and oxygen barrier properties of the BPT films. These interactions were analyzed by FTIR and X-ray diffraction analysis and their respective spectral and diffraction patterns are depicted in Fig. 9A and 9B. Apart from the characteristic peaks of native BP starch, the film (BP S) sample showed an increase in the intensity of the 1022 cm^{-1} band, which corresponds to the gelatinization of starch during the preparation of film matrix solution (Huang et al., 2021; Pozo et al., 2018). The increase in intensities of superimposed bands in 1046 and 1019 cm-1, were also noted in BP S films, which corresponds to the retrogradation of starch (Warren et al., 2016). The retrogradated starch films showed characteristic crystalline XRD diffraction peaks at 17.2, 20 and 22.3°, conforming to the B-type starch polymorph (Huang et al., 2021). The nanocellulose reinforced starch films (BP S + C) showed further increase in the intensity of characteristic band at 1022 cm^{-1} (Corresponding to glycosidic linkages), which may also be attributed to the high crystalline nature of nanocellulose fibers. The XRD diffraction pattern of cellulose reinforced films also emulated a similar result with high intensity crystalline peak around 22°. The reinforcement of nanocellulose fibers increased the overall crystallinity index of BP starch films from 20% to 48%.

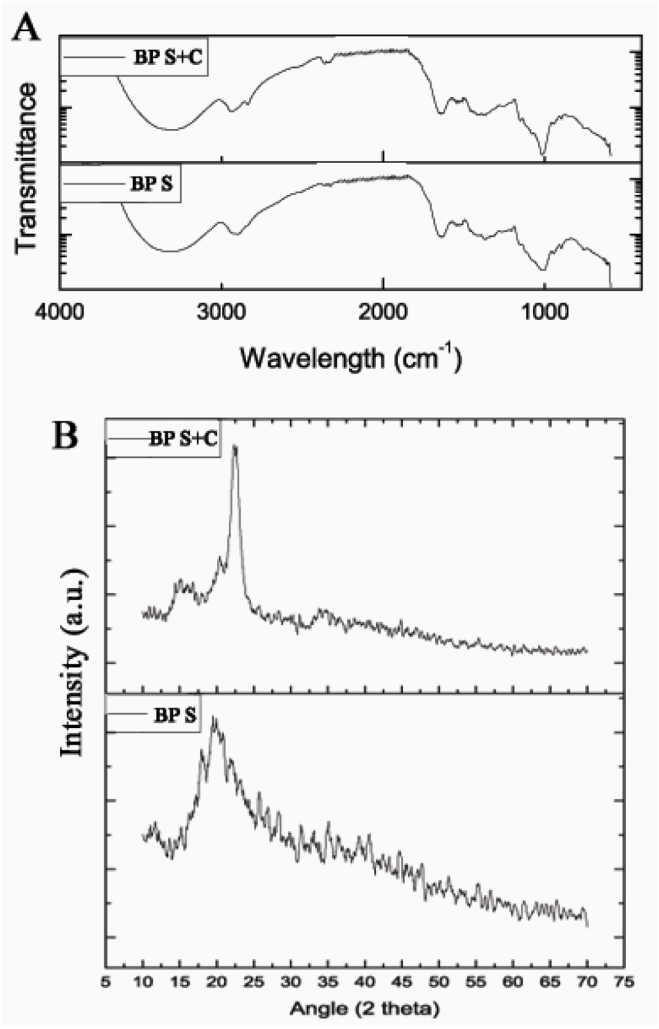

Fig. 9. A) FTIR spectroscopic pattern of BPT films; B) X-ray Diffraction pattern of BPT films [BP S – Banana Peel starch Film; BP S + C – Banana Peel cellulose reinforced starch film].

3.4. Production and characterization of bioactive BPT films

The optimized film matrix solution of 7.5%(w/v) BP starch and 3% (w/v) BP-NCF activated by 1.25%(w/v) citric acid was mixed with 150 μg/mL (MIC) of ethanolic extract of peel samples to produce bioactive BPT films. The bioactive BPT films were analyzed for antioxidant and antimicrobial properties. The DPPH inhibition assay of bioactive BPT films was examined to be 61.34 ± 0.71%. The antimicrobial inhibition zones of bioactive BPT films were 8.38 ± 0.24, 6.57 ± 0.12, 14.28 ± 0.14, 3.11 ± 0.12, 13.17 ± 0.21, and 18.22 ± 0.16 mm against *Listeria monocytogenes, Staphylococcus aureus, Escherichia coli, Klebsiella pneumonia*, and *Salmonella enteritidis, Pseudomonas aeruginosa,* respectively. From the above results, it is evident that the antimicrobial and antioxidant potential of bioactive BPT films is significantly lower than the innate potential of banana peel ethanolic extract. The starch molecules are prone to microbial contamination since they serve as a good carbon source for microbial growth. Consecutively, the antioxidant and antimicrobial potential of banana peel ethanolic extract was reduced in BPT films, which could be because of starch in BPT film (Harini et al., 2018).

Ultraviolet radiation from the sun can penetrate the packaging films and can initiate the oxidation of lipids in food. This leads to the rancidity of food products, especially in fat-rich food. Therefore, the UV-blocking property of the packaging films needs to be evaluated and enhanced to protect food products from UV radiation (Mehta & Kumar, 2019). Fig. 10A depicts the ultraviolet transmission spectra of BPT films. The BP starch-based film showed less UV blocking capacity with a transmittance percentage of 10.52 ± 0.85 and 8.47 ± 0.54%, respectively against UVA and UVB radiations. The nanocellulose reinforced BPT films showed a moderate UV blocking capacity of 95.31 ± 0.48% against both UVA and UVB radiations. The addition of bioactive compounds into BPT films significantly improved the UV blocking capacity of the films to ~98%. This may be attributed to phenolic components present in BP bioactive extract incorporated into the BPT films. Similar observations were noted by the addition of tea extracts in cellulose-based films by Shao et al. (2022).

The packaging materials should have good thermal stability to be used in harsh temperature conditions. Thus, the thermal stability of the BPT films was analyzed by thermogravimetric analysis, and the results are depicted in Fig. 10B. The initial weight loss till 150 °C corresponds to the removal of associated moisture content in the films (Weligama Thuppahige et al., 2023). The maximum degradation temperature for BP starch films was examined to be 290 °C, which is low compared to native BP starch. This may be attributed to the gelatinization and retrogradation of starch molecules in high water content for the production of BPT films (Huang et al., 2021). The citric acid crosslinking of cellulose into starch matrix has improved the thermal stability of the films, with 12 °C increases in maximum degradation temperature (302 °C). The addition of bioactive compounds didn't show much of an impact on the maximum degradation temperature of cellulose reinforced starch-based films, but there was a 5 °C reduction in starting point of degradation. This may be attributed to the dissociation of active compounds from the films.

3.5. Effect of bioactive BPT films on the shelf life of bread

Bread is one of the stable foods all over the world, freshly made bread without preservatives has very less shelf life (Dopazo et al., 2023). The effect of developed Bioactive BPT packages on the shelf-life parameters of bread stored at 4 °C is tabulated in Table 5. The initial moisture content of the sample was estimated to be 27.86 ± 0.53%. The moisture content of the bread significantly decreased throughout the storage period for all the samples. The reduction in moisture content of the samples packed in BPT and Bioactive BPT films was examined to be

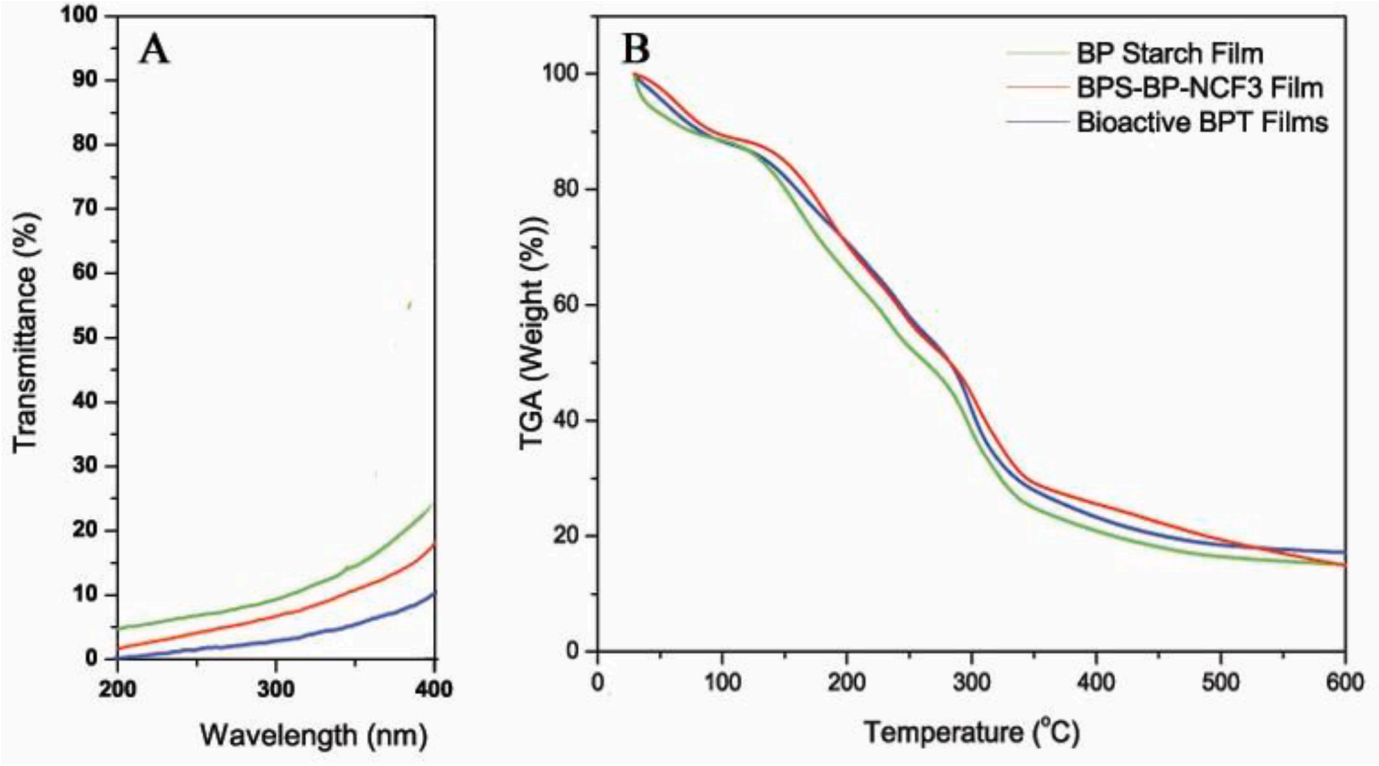

Fig. 10. A: Ultraviolet transmission spectra of BPT films; B: Thermogravimetric pattern of BPT films.

Table 5
Effect of Bioactive BPT packaging films on the Shelf life of bread stored at 4 °C.

Moisture content (%)	Bread Samples	Day 0			Day 5			Day 10			Day 15		
	PE	27.86 ± 0.53			23.65 ± 0.24			19.44 ± 0.52			16.34 ± 0.29		
	BPT	27.86 ± 0.53			22.04 ± 0.41			17.83 ± 0.28			14.21 ± 0.31		
	Bioactive BPT	27.86 ± 0.53			22.32 ± 0.33			17.95 ± 0.37			14.33 ± 0.25		
Water activity	PE	0.87 ± 0.02			0.85 ± 0.01			0.81 ± 0.06			0.79 ± 0.03		
	BPT	0.87 ± 0.02			0.82 ± 0.05			0.78 ± 0.03			0.73 ± 0.02		
	Bioactive BPT	0.87 ± 0.02			0.83 ± 0.04			0.78 ± 0.06			0.74 ± 0.04		
Texture/ Firmness [Fmax (N)]	PE	207.93 ± 0.54			226.35 ± 0.32			251.63 ± 0.41			270.41 ± 0.48		
	BPT	207.93 ± 0.54			237.12 ± 0.28			260.16 ± 0.37			286.32 ± 0.29		
	Bioactive BPT	207.93 ± 0.54			234.48 ± 0.35			256.83 ± 0.27			280.54 ± 0.62		
Color		L	a	b	L	A	b	L	a	b	L	a	b
	PE	84.27 ± 0.16	2.86 ± 0.22	19.32 ± 0.28	82.12 ± 0.12	−1.01 ± 0.19a	16.22 ± 0.23	80.36 ± 0.25	−1.57 ± 0.34a	14.31 ± 0.22	78.26 ± 0.37	−1.91 ± 0.18	12.68 ± 0.25
	BPT	84.27 ± 0.16	2.86 ± 0.22	19.32 ± 0.28	78.37 ± 0.27	−1.12 ± 0.16a	17.64 ± 0.28	74.28 ± 0.31	−1.82 ± 0.37a	15.43 ± 0.36	71.41 ± 0.41	−2.64 ± 0.22	13.23 ± 0.31
	Bioactive BPT	84.27 ± 0.16	2.86 ± 0.22	19.32 ± 0.28	82.69 ± 0.23	2.57 ± 0. 25b	18.26 ± 0.14	80.26 ± 0.28	2.11 ± 0.21b	16.75 ± 0.18	75.15 ± 0.33	−1.97 ± 0.28	13.50 ± 0.37
Acidity (%)	PE	1.35 ± 0.31			1.54 ± 0.27			1.78 ± 0.31[a]			2.57 ± 0.35[a]		
	BPT	1.35 ± 0.31			1.55 ± 0.18			1.80 ± 0.29[a]			2.55 ± 0.19[a]		
	Bioactive BPT	1.35 ± 0.31			1.39 ± 0.26			1.47 ± 0.37[b]			1.98 ± 0.33[b]		
Total Plate Count (Log CFU/g)	PE	3.81 ± 0.43			4.92 ± 0.38			5.81 ± 0.26			6.93 ± 0.33		
	BPT	3.81 ± 0.43			5.14 ± 0.29			5.98 ± 0.21			7.44 ± 0.29		
	Bioactive BPT	3.81 ± 0.43			4.25 ± 0.35			5.16 ± 0.32			6.55 ± 0.37		
Yeast and Mold (Log CFU/g)	PE	< 1			4.21 ± 0.18[a]			6.62 ± 0.26[a]			7.86 ± 0.22[a]		
	BPT	< 1			4.39 ± 0.25[a]			6.56 ± 0.22[a]			7.93 ± 0.31[a]		
	Bioactive BPT	< 1			< 1[b]			1.82 ± 0.31[b]			5.41 ± 0.28[b]		

Results are expressed in Mean ± S.D.
a - b, represents significant differences ($P < 0.05$) between values.

significantly ($P < 0.05$) high in comparison with samples stored in PE films. This may be attributed to the low moisture barrier properties of the starch-based thermoplastic films. Water activity is the measure of free moisture present in food and it is one of the main parameters, which defines the shelf life of food products. The growth of microorganisms in food is directly proportional to the water activity of the food, since microorganisms depend on the free water molecules in food for their growth (Chang et al., 2023; Dopazo et al., 2023). The initial water activity of bread samples was estimated to be 0.87 ± 0.02, which attributes to the initial bacterial count (total plate count) of 3.81 ± 0.43 Log CFU/g and (yeast and mold) count of < 1 Log CFU/g. Both PE and BPT packed bread samples showed similar growth patterns for bacterial and (yeast and mold) counts. The growth pattern of both bacteria and (yeast and mold) were examined to be significantly ($P < 0.05$) low for bread samples stored in Bioactive BPT packages. This significant reduction in microbial growth may be attributed to the high antimicrobial properties of active compounds present in Bioactive BPT packages. The shelf-life of bread depends on the visual observation of mold growth (Chang et al., 2023; Petchwattana et al., 2021). The bread samples packed in PE and BPT packages showed visual mold growth on the 5th day of storage, and the bread samples packed in Bioactive BPT packages showed visual mold growth on the 15th day of storage. Thus, the shelf life of bread is extended to a conservative estimate of 10 days in Bioactive BPT packages, without any addition of chemical preservatives. All the bread samples showed a significant ($P < 0.05$) increase in titratable acidity with storage days. This may be attributed to the growth of lactobacillus in bread samples (Dopazo et al., 2023). The texture and color of the food products are driving factors for consumer acceptance. The initial color and firmness of the bread samples were examined to be [84.27 ± 0.16 (L - Light), 2.86 ± 0.22 (a - red), 19.32 ± 0.28 (b - yellow)] and 207.93 ± 0.54 N, respectively. The firmness of all the samples was examined to significantly ($P < 0.05$) increase with storage days, attributing to the reduction in moisture content of the bread. All the bread samples showed significant ($P < 0.05$) reduction in Lightness, redness and yellowness with storage days. Both PE and BPT packed bread samples showed an increase in greenness after 5th day of storage. Similarly, bread samples packed in Bioactive BPT films also showed greenness on the 15th day of storage, attributed to the visual growth of molds.

4. Conclusions

The active compounds present in banana peels showed high antioxidant and antimicrobial properties. Consecutively, they serve as a potential replacement for synthetic active compounds to develop food packaging aids. The banana peel starch molecules were examined to be rich in amorphous amylopectin molecules, which serve as a potential matrix for the development of starch-based thermoplastic films. The nanocellulose fibers produced from banana peel exhibited superior reinforcing capabilities that influence the mechanical and barrier characteristics of BPT films. In conclusion, the banana peels collected from the banana processing industries have the potential to produce bioactive thermoplastics packaging films. We believe that this work will give a positive impact on the journey to achieve bio circular economy in banana processing industries. The bioactive BPT packages were examined to be effective in increasing the shelf-life of bread up to 10 days at a storage temperature of 4 °C, without any chemical preservatives. In future research perspectives, the produced bioactive BPT films have to be subjected to degradation kinetic studies in the soil to serve as organic content enhancers (nutrients for beneficial soil microbes).

Declaration of Competing Interest

The authors declare that they have no known competing financial interests or personal relationships that could have appeared to influence the work reported in this paper.

Data availability

No data was used for the research described in the article.

Acknowledgement

The first author would like to recognize the Council of Scientific and Industrial Research – CSIR for the fellowship grant (No.:09/468/0500/2016/EMR-I).

References

Acharya, S., Hu, Y., Moussa, H., & Abidi, N. (2017). Preparation and characterization of transparent cellulose films using an improved cellulose dissolution process. *Journal of Applied Polymer Science, 134*(21). https://doi.org/10.1002/app.44871

Alamri, M. S., Mohamed, A. A., & Hussain, S. (2012). Effect of okra gum on the pasting, thermal, and viscous properties of rice and sorghum starches. *Carbohydrate Polymers, 89*, 199–207. https://doi.org/10.1016/j.carbpol.2012.02.071

Algar, A. F. C., Umali, A. B., & Tayobong, R. R. P. (2019). Physicochemical and functional properties of starch from philippine edible canna (Canna indica L.) rhizomes. *Journal of Microbiology, Biotechnology and Food Sciences, 9*(1). https://doi.org/10.15414/JMBFS.2019.9.1.34-37

Chandra Mohan, C., Harini, K., Vajiha Aafrin, B., Lalitha priya, U., Maria jenita, P., Babuskin, S., Karthikeyan, S., Sudarshan, K., Renuka, V., & Sukumar, M. (2018). Extraction and characterization of polysaccharides from tamarind seeds, rice mill residue, okra waste and sugarcane bagasse for its Bio-thermoplastic properties. *Carbohydrate Polymers, 186*(December 2017), 394–401. https://doi.org/10.1016/j.carbpol.2018.01.057

Chang, Y. H., Chang, C. M., & Chuang, P. T. (2023). Shelf-life assessment of bread partially substituted with soy protein isolate. *Applied Sciences (Switzerland), 13*(6). https://doi.org/10.3390/app13063960

Coates, J. (2006). Interpretation of infrared spectra, a practical approach. Encyclopedia of Analytical Chemistry (pp. 10815–10837). https://doi.org/10.1002/9780470027318.a5606.

Czaikoski, A., da Cunha, R. L., & Menegalli, F. C. (2020). Rheological behavior of cellulose nanofibers from cassava peel obtained by combination of chemical and physical processes. *Carbohydrate Polymers, 248*. https://doi.org/10.1016/j.carbpol.2020.116744

Deepa, B., Abraham, E., Pothan, L. A., Cordeiro, N., Faria, M., & Thomas, S. (2016). Biodegradable nanocomposite films based on sodium alginate and cellulose nanofibrils. *Materials*. https://doi.org/10.3390/ma9010050

Dopazo, V., Illueca, F., Luz, C., Musto, L., Moreno, A., Calpe, J., & Meca, G. (2023). Evaluation of shelf life and technological properties of bread elaborated with lactic acid bacteria fermented whey as a bio-preservation ingredient. *LWT, 174*. https://doi.org/10.1016/j.lwt.2023.114427

dos Santos, T. P. R., Leonel, M., Garcia, É. L., do Carmo, E. L., & Franco, C. M. L. (2016). Crystallinity, thermal and pasting properties of starches from different potato cultivars grown in Brazil. *International Journal of Biological Macromolecules*. https://doi.org/10.1016/j.ijbiomac.2015.10.091

Eyholzer, C., Bordeanu, N., Lopez-Suevos, F., Rentsch, D., Zimmermann, T., & Oksman, K. (2010). Preparation and characterization of water-redispersible nanofibrillated cellulose in powder form. *Cellulose (London, England)*. https://doi.org/10.1007/s10570-009-9372-3

Ferreira, D. C. M., Molina, G., & Pelissari, F. M. (2020). Biodegradable trays based on cassava starch blended with agroindustrial residues. *Composites Part B: Engineering, 183*. https://doi.org/10.1016/j.compositesb.2019.107682

Ghasemlou, M., Aliheidari, N., Fahmi, R., Shojaee-Aliabadi, S., Keshavarz, B., Cran, M. J., & Khaksar, R. (2013a). Physical, mechanical and barrier properties of corn starch films incorporated with plant essential oils. *Carbohydrate Polymers, 98*, 1117–1126. https://doi.org/10.1016/j.carbpol.2013.07.026

Ghasemlou, M., Aliheidari, N., Fahmi, R., Shojaee-Aliabadi, S., Keshavarz, B., Cran, M. J., & Khaksar, R. (2013b). Physical, mechanical and barrier properties of corn starch films incorporated with plant essential oils. *Carbohydrate Polymers*. https://doi.org/10.1016/j.carbpol.2013.07.026

Han, J. H., & Floros, J. D. (1997). Casting antimicrobial packaging films and measuring their physical properties and antimicrobial activity. *Journal of Plastic Film and Sheeting*. https://doi.org/10.1177/875608799701300405

Harini, K., Chandra Mohan, C., Ramya, K., Karthikeyan, S., & Sukumar, M. (2018a). Effect of Punica granatum peel extracts on antimicrobial properties in Walnut shell cellulose reinforced Bio-thermoplastic starch films from cashew nut shells. *Carbohydrate Polymers, 184*, 231–242. https://doi.org/10.1016/j.carbpol.2017.12.072

Harini, K., Ramya, K., & Sukumar, M. (2018b). Extraction of nano cellulose fibers from the banana peel and bract for production of acetyl and lauroyl cellulose. *Carbohydrate Polymers, 201*(June), 329–339. https://doi.org/10.1016/j.carbpol.2018.08.081

Hassan, M. M., Tucker, N., & Le Guen, M. J. (2020). Thermal, mechanical and viscoelastic properties of citric acid-crosslinked starch/cellulose composite foams. *Carbohydrate Polymers, 230*. https://doi.org/10.1016/j.carbpol.2019.115675

Hassan, Z., Jahan, I., Saha, G., Begum, F., Nada, K., & Choudhury, J. (1970). Studies on the peel oil from two varieties of banana. *Bangladesh Journal of Scientific and Industrial Research*. https://doi.org/10.3329/bjsir.v45i4.7387

Hizukuri, S., Kaneko, T., & Takeda, Y. (1983). Measurement of the chain length of amylopectin and its relevance to the origin of crystalline polymorphism of starch granules. *BBA - General Subjects*. https://doi.org/10.1016/0304-4165(83)90142-3

Huang, S., Chao, C., Yu, J., Copeland, L., & Wang, S. (2021). New insight into starch retrogradation: The effect of short-range molecular order in gelatinized starch. *Food Hydrocolloids, 120*. https://doi.org/10.1016/j.foodhyd.2021.106921

Iyer, K. A., Zhang, L., & Torkelson, J. M. (2016). Direct use of natural antioxidant-rich agro-wastes as thermal stabilizer for polymer: Processing and recycling. *ACS Sustainable Chemistry and Engineering*. https://doi.org/10.1021/acssuschemeng.5b00945

Jafari, E., Jarah-Najafabadi, N. T., Jahanian-Najafabadi, A., Poorirani, S., Hassanzadeh, F., & Sadeghian-Rizi, S. (2017). Synthesis and evaluation of antimicrobial activity of cyclic imides derived from phthalic and succinic anhydrides. *Research in Pharmaceutical Sciences*. https://doi.org/10.4103/1735-5362.217433

Abdul Khalil, H.P. S., Bhat, A.H., & Ireana Yusra, A F. (2012). Green composites from sustainable cellulose nanofibrils: A review. In Carbohydrate Polymers. https://doi.org/10.1016/j.carbpol.2011.08.078.

Kumar, A., Negi, Y. S., Choudhary, V., & Bhardwaj, N. K. (2014). Characterization of cellulose nanocrystals produced by acid-hydrolysis from sugarcane bagasse as agro-waste. *Journal of Materials Physics and Chemistry*. https://doi.org/10.12691/jmpc-2-1-1

Li, M. C., Wu, Q., Song, K., Lee, S., Qing, Y., & Wu, Y. (2015). Cellulose nanoparticles: Structure-morphology-rheology relationships. *ACS Sustainable Chemistry and Engineering, 3*, 821–832. https://doi.org/10.1021/acssuschemeng.5b00144

Maya, M. G., George, S. C., Jose, T., Sreekala, M. S., & Thomas, S. (2017). Mechanical properties of short sisal fibre reinforced phenol formaldehyde eco-friendly composites. *Polymers from Renewable Resources*. https://doi.org/10.1177/204124791700800103

Mehta, M. J., & Kumar, A. (2019). Ionic liquid assisted gelatin films: Green, UV Shielding, antioxidant, and antibacterial food packaging materials. *ACS Sustainable Chemistry and Engineering, 7*(9). https://doi.org/10.1021/acssuschemeng.9b00423

Mordi, R. C., Fadiaro, A. E., Owoeye, T. F., Olanrewaju, I. O., Uzoamaka, G. C., & Olorunshola, S. J. (2016). Identification by GC-MS of the components of oils of banana peels extract, phytochemical and antimicrobial analyses. *Research Journal of Phytochemistry*. https://doi.org/10.3923/rjphyto.2016.39.44

Nagarajaiah, S. B., & Prakash, J. (2011). Chemical composition and antioxidant potential of peels from three varieties of banana. *Asian Journal of Food and Agro-Industry*. https://doi.org/10.1016/0309-1740(95)80016-6

Ododo, M. M., Choudhury, M. K., & Dekebo, A. H. (2016). Structure elucidation of β-sitosterol with antibacterial activity from the root bark of Malva parviflora. *SpringerPlus*. https://doi.org/10.1186/s40064-016-2894-x

Pérez, S., & Bertoft, E. (2010). The molecular structures of starch components and their contribution to the architecture of starch granules: A comprehensive review. In *Starch/Staerke* (Vol. 62, Issue 8). https://doi.org/10.1002/star.201000013.

Petchwattana, N., Naknaen, P., Cha-aim, K., Suksri, C., & Sanetuntikul, J. (2021). Controlled release antimicrobial sachet prepared from poly(butylene succinate)/geraniol and ethylene vinyl alcohol coated paper for bread shelf-life extension application. *International Journal of Biological Macromolecules, 189*, 251–261. https://doi.org/10.1016/j.ijbiomac.2021.08.119

Pozo, C., Rodríguez-Llamazares, S., Bouza, R., Barral, L., Castaño, J., Müller, N., & Restrepo, I. (2018). Study of the structural order of native starch granules using combined FTIR and XRD analysis. *Journal of Polymer Research, 25*(12). https://doi.org/10.1007/s10965-018-1651-y

Puncha-Arnon, S., & Uttapap, D. (2013). Rice starch vs. rice flour: Differences in their properties when modified by heat-moisture treatment. *Carbohydrate Polymers, 91*, 85–91. https://doi.org/10.1016/j.carbpol.2012.08.006

Radha Krishnan, K. (2015). *Predective preservative model for the shelf life of meat chain*. Anna University. http://hdl.handle.net/10603/43011.

Saberi, B., Thakur, R., Bhuyan, D. J., Vuong, Q. V., Chockchaisawasdee, S., Golding, J. B., Scarlett, C. J., & Stathopoulos, C. E. (2017). Development of edible blend films with good mechanical and barrier properties from pea starch and guar gum. *Starch/Staerke*. https://doi.org/10.1002/star.201600227

Sahoo, P. K., Mohapatra, R., Sahoo, A., DebSarkar, N., & Swain, S. K. (2005). Characterization, biodegradation, and water absorbency of chemically modified tossa variety jute fiber via pulping and grafting with acrylamide. *International Journal of Polymer Analysis and Characterization*. https://doi.org/10.1080/10236660500397845

Sakkas, H., & Papadopoulou, C. (2017). Antimicrobial activity of basil, oregano, and thyme essential oils. *Journal of Microbiology and Biotechnology, 27*(3), 429–438. https://doi.org/10.4014/jmb.1608.08024

Sen, A., Dhavan, P., Shukla, K. K., Singh, S., & Tejovathi, G. (2012). Analysis of IR, NMR and antimicrobial activity of β-sitosterol isolated from Momordica charantia. *Science Secure Journal of Biotechnology, 1*, 9–13.

Shao, H., Zhang, Y., Pan, H., Jiang, Y., Qi, J., Xiao, H., Zhang, S., Lin, T., Tu, L., & Xie, J. (2022). Preparation of flexible and UV-blocking films from lignin-containing cellulose incorporated with tea polyphenol/citric acid. *International Journal of Biological Macromolecules, 207*, 917–926. https://doi.org/10.1016/j.ijbiomac.2022.03.183

Sudharsan, K., Chandra Mohan, C., Azhagu Saravana Babu, P., Archana, G., Sabina, K., Sivarajan, M., & Sukumar, M. (2016). Production and characterization of cellulose reinforced starch (CRT) films. *International Journal of Biological Macromolecules, 83*, 385–395. https://doi.org/10.1016/j.ijbiomac.2015.11.037

Sui, Z., Yao, T., Ye, X., Bao, J., Kong, X., & Wu, Y. (2016). Physicochemical properties and starch digestibility of in-kernel heat-moisture treated waxy, low and high-amylose rice starch. *Starch/Staerke, 69*, 7–8.

Tibolla, H., Pelissari, F. M., Martins, J. T., Vicente, A. A., & Menegalli, F. C. (2018). Cellulose nanofibers produced from banana peel by chemical and mechanical treatments: Characterization and cytotoxicity assessment. *Food Hydrocolloids, 75*, 192–201. https://doi.org/10.1016/j.foodhyd.2017.08.027

Tibolla, H., Pelissari, F. M., & Menegalli, F. C. (2014). Cellulose nanofibers produced from banana peel by chemical and enzymatic treatment. *LWT - Food Science and Technology, 59*, 1311–1318. https://doi.org/10.1016/j.lwt.2014.04.011

van Soest, J. J. G., Tournois, H., de Wit, D., & Vliegenthart, J. F. G. (1995). Short-range structure in (partially) crystalline potato starch determined with attenuated total reflectance Fourier-transform IR spectroscopy. *Carbohydrate Research, 279*(C). https://doi.org/10.1016/0008-6215(95)00270-7

Veiga-Santos, P., Oliveira, L. M., Cereda, M. P., Alves, A. J., & Scamparini, A. R. P. (2005). Mechanical properties, hydrophilicity and water activity of starch-gum films: Effect of additives and deacetylated xanthan gum. *Food Hydrocolloids, 19*(2), 341–349. https://doi.org/10.1016/j.foodhyd.2004.07.006

Warren, F. J., Gidley, M. J., & Flanagan, B. M. (2016). Infrared spectroscopy as a tool to characterise starch ordered structure - A joint FTIR-ATR, NMR, XRD and DSC study. *Carbohydrate Polymers, 139*. https://doi.org/10.1016/j.carbpol.2015.11.066

Weligama Thuppahige, V. T., Moghaddam, L., Welsh, Z. G., Wang, T., Xiao, H.-. W., & Karim, A. (2023). Extraction and characterisation of starch from cassava (Manihot esculenta) agro-industrial wastes. *LWT, 182*, Article 114787. https://doi.org/10.1016/j.lwt.2023.114787

Wilpiszewska, K., & Czech, Z. (2014). Citric acid modified potato starch films containing microcrystalline cellulose reinforcement - Properties and application. *Starch/Staerke, 66*(7–8). https://doi.org/10.1002/star.201300093

Wulandari, W. T., Rochliadi, A., & Arcana, I. M. (2016). Nanocellulose prepared by acid hydrolysis of isolated cellulose from sugarcane bagasse. In *IOP Conference Series: Materials Science and Engineering*. https://doi.org/10.1088/1757-899X/107/1/012045

Yuliana, M., Huynh, L. H., Ho, Q. P., Truong, C. T., & Ju, Y. H. (2012). Defatted cashew nut shell starch as renewable polymeric material: Isolation and characterization. *Carbohydrate Polymers*. https://doi.org/10.1016/j.carbpol.2011.11.044

Zobel, H. F. (1988). Starch crystal transformations and their industrial importance. *Starch - Stärke*. https://doi.org/10.1002/star.19880400102